Van Gurp-Palmen-plot: A way to characterize polydispersity of linear polymers

Article *in* Rheologica Acta · January 2001

DOI: 10.1007/s003970000137

2 authors, including:

Christian Friedrich
University of Freiburg
186 PUBLICATIONS **7,913** CITATIONS

SEE PROFILE

Rheol Acta (2001) 40: 322–328

ORIGINAL CONTRIBUTION

Stefan Trinkle
Christian Friedrich

Van Gurp-Palmen-plot: a way to characterize polydispersity of linear polymers

Received: 25 July 2000
Accepted: 25 October 2000

S. Trinkle · C. Friedrich (✉)
Institut für Makromolekulare Chemie
Albert-Ludwig-Universität Freiburg
Stefan-Meier Str. 31
79104 Freiburg i. Br., Germany
e-mail: chf@fmf.uni-freiburg.de

Abstract This article is concerned with the so-called van Gurp-Palmen-plot which charts the phase angles vs the absolute values of the complex shear modulus from a rheological experiment. Its basic characteristic features are elucidated for polymers having a simple, i.e., a linear structure. A subsequent manuscript will then address more complicated topologies as present in long chain branched polymers.

A unique type of curve is typical for linear samples. This type of curve is characterized by one minimum and one inflection point. The locations of these points and thus the shape of the curve are correlated to the plateau modulus, to the molecular weight, and, especially, to the polydispersity. With these findings in mind, scaling is then introduced to the van Gurp-Palmen-plot. Finally, bimodal homopolymer blends are considered in order to learn how two distinct relaxation processes influence the shape of the van Gurp-Palmen-plot.

Key words Rheology · van Gurp-Palmen-plot · Molecular topology · Polydispersity · Plateau modulus

Introduction

Van Gurp and Palmen (1998) presented in a rarely noticed publication an approach for the verification of the time temperature superposition principle (TTS). They plotted the phase angle δ of the measured rheological data vs the corresponding absolute value of the complex shear modulus $|G^*|$ and found that isothermal frequency curves merge into a common line if the TTS holds. In the following we will call this plot the van Gurp-Palmen-plot (vGP-plot). This way of verifying the TTS principle for a given polymer sample is based on the exclusion of the temperature-dependent characteristic elementary time τ_0 and the quantities deduced from τ_0 according to the scaling laws (Doi and Edwards 1986). Equivalent conclusions were also drawn by others, for example by Mavridis and Shroff (1992), who used the loss tangent, tan δ, instead of the phase angle δ itself.

Applying the method of van Gurp and Palmen and working with the plot, we found that it comprises even more information about, e.g., polydispersity and long chain branching (LCB). However, before turning to LCB we have to explore the fundamental influence of molecular characteristics of linear polymers like molecular weight (MW), MW-distribution (MWD), tacticity, and chemical composition (in case of copolymers) on the shape of the curve in the vGP-plot. Some fundamental conclusions will be drawn from the consideration of bimodal homopolymer blends. In a subsequent article we will focus on the characteristics of long chain branched samples.

In general, we are trying to establish the vGP-plot as a useful and reliable tool for characterizing a sample's melt properties.

Experimental

Materials

Poly(styrene) (PS) and poly(methylmethacrylate) (PMMA). The samples have been prepared by anionic polymerization and are typically monodisperse. The synthesis is described elsewhere (Eckstein 1998; Fuchs et al. 1996). The physical data of interest in this paper are charted in Table 1.

Poly(olefin)s. The polymers under investigation are metallocene poly(olefin)s with varying molar masses and typical polydispersities between 2 and 2.5 – see Tables 2 and 3. The synthesis and characterization of the considered samples are described in detail elsewhere (Suhm 1998; Walter 1998). When necessary the polymers have been stabilized with antioxidants (Irganox/Irgaphos) against thermal degradation, chain extension, and/or scissoring, respectively.

Rheology

Dynamic data were obtained with either the Rheomotrics RMS 800 or with the Bohlin CVO 120 rheometer both equipped with 25-mm parallel plate geometry. The applied stresses or deformations were within the limits of linear viscoelasticity. Creep measurements at the reference temperature were done with those samples that had not reached the terminal flow region in oscillatory mode. The creep data were converted into the retardation time spectra L(λ) by the computer program *NLReg* (Honerkamp and Weese 1993a, b). Subsequently, the complex shear compliance J*(ω) was calculated from L(λ) (Ferry 1980) and the shear moduli G′ and G″ from J*(ω).The procedure is sketched in Fig. 1. With this procedure of combining oscillatory and creep measurements, master curves can be extended towards lower frequencies.

Results and discussion

Polymers with a linear topology (“*linears*”) have a unique course of curve in the vGP-plot like those given in Fig. 2. Moving from high to low modulus values the phase angle δ drops, passes a minimum, rises again, moves through an inflection point, and finally approaches its limiting value of 90°. This characteristic curvature is found for amorphous polymers such as poly(styrene). For crystalline polymers like poly(ethene) only the part on the left side of the minimum can be monitored by melt rheology, since crystallization occurs at the low temperatures that are necessary to reach the minimum region. For this reason the characteristics of linear polymers are demonstrated with poly(styrene). The 90° plateau in the vGP-plot is equivalent to the terminal flow range in the usual master curve plot and indicates viscous behavior. In the following we will focus on parameters such as plateau modulus, which is primarily governed by the chemical constitution of the polymer, tacticity, and copolymer composition. Then we will consider the molecular weight (MW), MW-distribution (MWD), as well as bimodality.

Polymer invariant representation: the reduced van Gurp-Palmen-plot

The van Gurp-Palmen-curves of several atactic polystyrene samples with varied molecular weights are plotted in Fig. 2. Apparently, the horizontal positions of the minima scatter around 2 × 10^5 Pa, which is the value of the poly(styrene) plateau modulus G_N^0 (Donth 1992). This finding can be reasoned by a mathematical consideration. The plateau modulus is defined by Eq. (1):

$$G_N^0 = G'\left(\omega|_{\tan\delta \text{ at min}}\right) \tag{1}$$

Table 1 Characteristic data of the poly(styrene) and the poly(methylmethacrylate) series under investigation

	PS55	PS60	PS120	PS140	PS180	PS240	PS427	PS6440	PS1600	PMM-A71	PMM-A145	PMM-A170	PMM-A390
M_n[kg/mol]	51	68	116	137	174	230	396	591	1400	65	138	140	350
M_w[kg/mol]	54	71	120	141	181	240	427	644	1600	71	145	170	390
PD = M_w/M_n	1.05	1.05	1.05	1.03	1.04	1.05	1.08	1.09	1.15	1.06	1.05	1.17	1.14

Table 2 Characteristic data of the poly(olefin) polymers with a linear molecular topology

	PE01	PE03	PE04	PE05	iPP109	sPP103	aPP3600	PB131	PE400
M_n[kg/mol]	80	34	25	72	62	61	1890	47	80
M_w[kg/mol]	249	230	249	251	109	103	3670	131	249
PD = M_w/M_n	3.1	6.6	9.7	3.5	1.8	1.7	1.9	2.8	3.1

Table 3 Characteristic data of the poly(ethene-*co*-propene) polymers with a linear molecular topology

	(EP39)96 39 wt% propene	(EP39)64 68 wt% propene	(EP39)80 75 wt% propene	(EP39)94 84 wt% propene	(EP39)300 95 wt% propene	(EP39)1163 97 wt% propene
M_n[kg/mol]	46	32	39	49	111	52.5
M_w[kg/mol]	96	64	80	84	300	116
PS = M_w/M_n	2.1	2.0	2.1	1.9	2.7	2.2

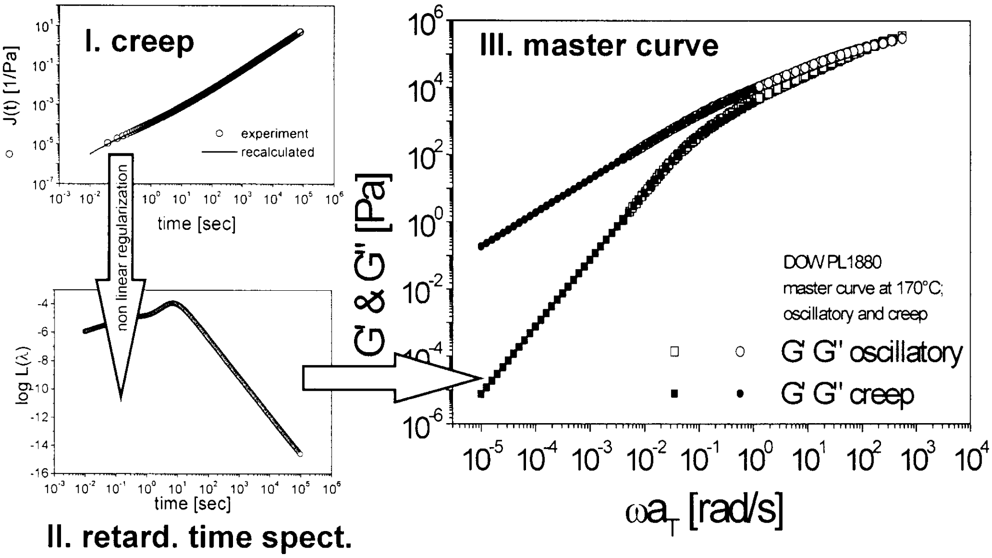

Fig. 1 Extending the experimental window towards lower frequencies by combining creep and oscillatory measurements

This definition can be expressed in terms of $|G^*(\delta)|$:

$$G_N^0 = \lim_{\delta \to 0} |G^*(\delta)| \tag{2}$$

because, when $\delta \to 0$, then $\tan\delta \to 0$ (that is also the minimum, since negative δ do not have any physical relevance), G' dominates over G'' and finally disappears such that $|G^*|$ approaches G'. Therefore $|G^*|$ in the minimum equals the plateau modulus. Keeping this in mind it can be stated that the minimum in the vGP-plot is associated with the plateau modulus G_N^0 and the lower this minimum is located on the vertical axis, the more accurately does the $|G^*|$ value in the minimum correspond to the plateau modulus G_N^0. However, even for low molecular weight poly(styrene)s, $|G^*|_{\delta\text{-min}}$ is very close to G_N^0. Identical conclusions can be drawn from a series of narrowly distributed poly(methylmethacrylate), PMMA, samples with varied molar masses. These data were published by Fuchs et al. (1996). Thus, the vGP-plot is another possibility for the determination of the plateau modulus G_N^0.

Focusing on the characteristics of linear polymers in the vGP-plot it seems to be favorable to find a presentation which is independent of the polymer's chemical constitution, respectively its G_N^0 value. By dividing the absolute value of the shear moduli $|G^*|$ by G_N^0 one obtains a reduced presentation of the van Gurp-Palmen-plot (rvGP-plot, Fig. 3). Besides the

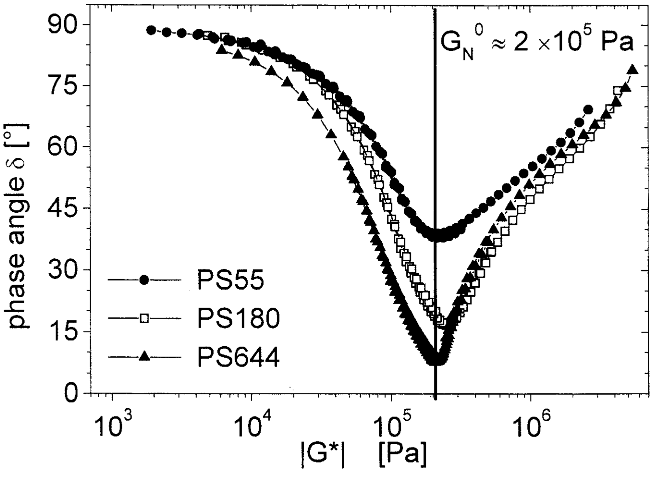

Fig. 2 The vGP-plots of three poly(styrene) samples with different molecular weights. The numbers following the acronym "*PS*" denotes the sample's molar mass in [kg/mol]. For reasons of clarity only three curves are plotted

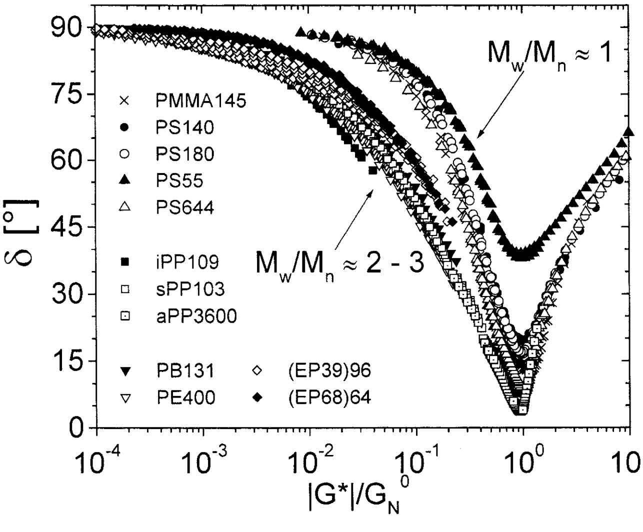

Fig. 3 RvGP-plots of polymers having different chemical compositions. Traces of polymers having the same polydispersity are on top of one another below a $|G^*|/G_N^0$ ratio of 10^{-1}

monodisperse poly(styrene) from Fig. 2, a set of poly(olefin)s having polydispersities between 2 and 3 are plotted in Fig. 3. Within the experimental error, all polymers with the same polydispersity superimpose, regardless of (i) tacticity and (ii) chemical nature (compare: (i) isotactic (iPP109) vs syndiotactic (sPP103) vs atactic poly(propene) (aPP3600) and (ii) poly(styrene) (PS140) vs poly(methylmethacrylate) (PMMA145) and polyethylene (PE400) vs poly(butene) PB131). The plateau moduli of the considered polymers were published by Eckstein et al. (1998) and by Donth (1992). Polydispersity and molecular weight are responsible for the fact that not all curves are on top of one another, as will be shown below in more detail. The important message of this section is that polymers of different chemical nature can be compared to one another.

If one wants to verify whether the previously obtained results are also applicable to metallocene type poly(olefin) copolymers, one encounters the problem that the plateau moduli of these materials are not always accessible by experimental means. In this section we will explain how G_N^0 can be determined anyway for olefin copolymers. Figure 4 shows the vGP-plots of several ethene/propene copolymers and reveals that the copolymer curves are embedded between those of the two homopolymers. The attempt to shift all curves on top of one another succeeds and the evaluation of the shift parameters yields in a linear log a_x vs x correlation with x being the composition in wt%. As a consequence the log $|G^*|$ values at any given δ depend linearly on composition. This is demonstrated in Fig. 5. Since this linearity is valid for any constant δ it is also given for $\delta = 0$, and $|G^*(\delta = 0)|$ is equals the plateau modulus G_N^0. With this consideration in mind and knowing the G_N^0 values of the homopolymers (Eckstein 1998; Donth 1992) one can calculate the plateau modulus for any composition. We did this for two poly(ethene-*co*-propene)s with a polydispersity of about 2, calculated the rvGP traces and added them to Fig. 3. These curves are located between those of PMMA145 (Mw/Mn = 1.05) and of PB131 (Mw/Mn = 2.8) in agreement with their polydispersity. These observations are in agreement with the known mixing laws by Wu and Beckerbauer (1992) and by Lobbrecht et al. (1997).

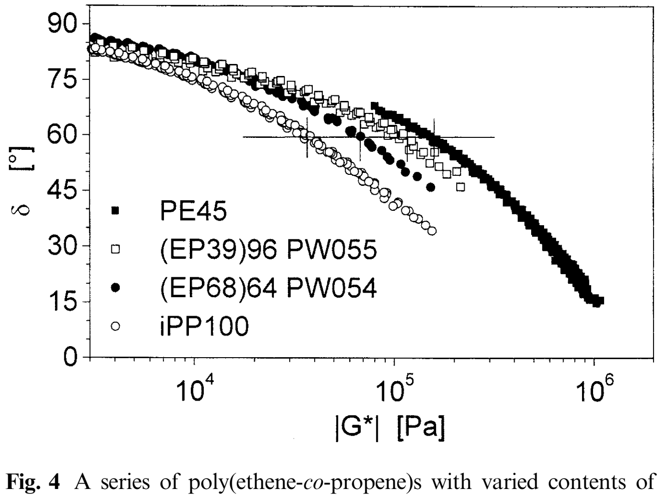

Fig. 4 A series of poly(ethene-*co*-propene)s with varied contents of propene

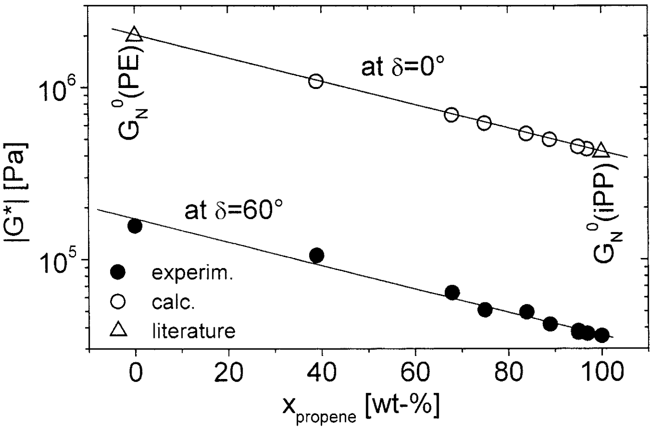

Fig. 5 A linear correlation is found between propene $x_{propene}$ content and the shear modulus $|G^*|$ at $\delta = 60°$. Analogously, G_N^0 can be calculated when knowing the plateau moduli of the homopolymers. G_N^0 (PE) and G_N^0 (iPP) in this plot are literature data

From the considerations so far it has become clear that the reduced van Gurp-Palmen-plot is valuable because it is independent of the characteristic elementary relaxation time τ_0, the temperature, chemical composition, and tacticity.

Influence of polymer topology on the rvGP-plot

Molecular weight. Figure 2 also reveals that the vertical position of the minimum correlates with the sample's molecular weight. A high molar mass sample passes the minimum at a lower phase angle δ than a low molecular mass probe does. This observation will be elucidated quantitatively in Fig. 6, in which the (M_w/M_e; δ_{min}) data pairs of the polymers of Fig. 2 and Table 1 are plotted. The molecular weight is expressed here by the multiple of the entanglement molecular weight M_e (Fuchs et al. 1996; Fetters et al. 1999). A linear correlation can be deduced and a linear regression gives $\log \delta_{min} = 1.91 - 0.61 \times \log M_w$ for poly(styrene) and $\delta_{min} = 2.08 - 0.72 \times \log M_w$ for poly(methylmethacrylate). Rather than treating the data for each polymer type separately (as we did) one could assume that Fig. 6 is polymer-type independent and the scatter of data points is statistical. This would mean that all data points fell onto a common line. The question of polymer-type independent scaling in Fig. 6 still remains open. Regardless of this, the vGP-plot is a possible route for determining a sample's molecular weight.

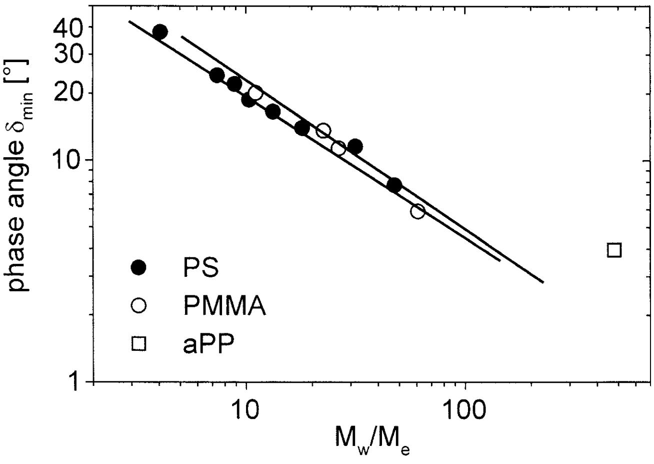

Fig. 6 The phase angle δ in the G_N^0-minimum vs relative molar mass for the series of poly(styrene)s and poly(methylmethacrylate). The lines indicate the results of linear regressions

While the curves in Fig. 2 deviate from one another in the G_N^0 region in dependence of their molar mass, they converge within approximately one decade below G_N^0 and finally become MW-independent in the 90° plateau. The deviation below $|G^*|/G_N^0$ values of 0.1 becomes negligible with high molar mass polymers whereas we apply here the overall accepted definition of a high molar mass polymer: one having a molecular weight of ten times M_e or higher.

Polydispersity. In Fig. 7 the influence of polydispersity on the vGP-plot is demonstrated. The samples are linear polymers with approximately the same molecular weight average (except (EP75)80) but different molecular weight distributions (Tables 1 and 2). As the degree of polydispersity increases the left flank of the vGP-plot becomes less steep and the terminal flow plateau at 90° is reached at lower values of $|G^*|$. Since poly(ethene) is capable of crystallizing the G_N^0 minimum usually cannot be reached for these samples. Towards higher values of $|G^*|$ the curves converge, leading to the conclusion that polydispersity does not change the type of curve (no additional inflection points etc.) but stretches the curves at low $|G^*|$ along the abscissa. This is quantitatively shown in Fig. 8, which is a log-log plot of the complex shear modulus at $\delta = 60^\circ$ vs the degree of polydispersity M_w/M_n $\delta = 60^\circ$ was chosen since the lines merge on one hand into a common point – the G_N^0 minimum – for $\delta \rightarrow \delta|_{min}$ and on the other hand into the terminal flow plateau towards 90°. From a phenomenological point of view maximum deviation of curves from one another is given best for $\delta = 60^\circ$. At this point it must be pointed out that Fig. 8 may be applied only to polymers with a molar mass well above their entanglement molecular weight, because then molecular weight effects are negligible. Then, Fig. 8 can be used to estimate a samples polydispersity.

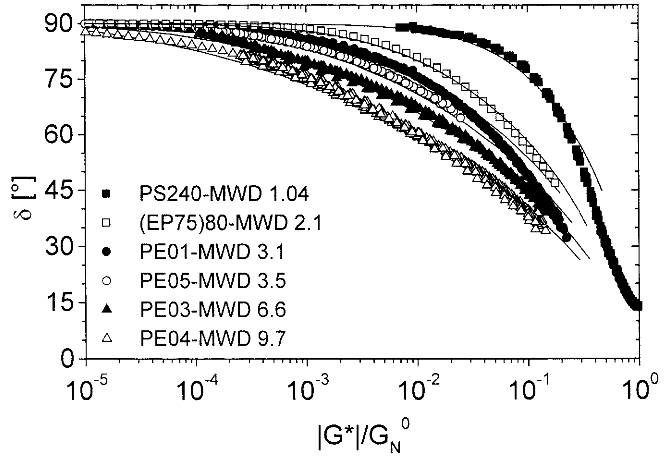

Fig. 7 The rvGP plot of samples with different polydispersity. The samples are linear poly(styrene) and high density poly(ethene)s with molar masses between 230 kg/mol and 251 kg/mol. EP(75)80 is a poly(ethene-*co*-propene) with 75 wt% propene. *Solid lines* indicate corresponding simulated data on basis of the double reptation model as described in the text

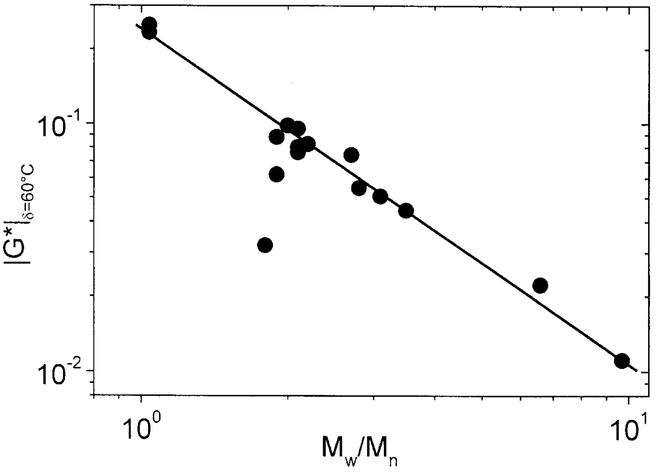

Fig. 8 Correlation between polydispersity and $|G^*|$-value at $\delta = 60^\circ$. The samples are those of Fig. 7 and Tables 2 and 3 as well as selected probes of Table 1

These observations are consistent with literature data by Kazatchkov et al. (1999) as well as with existing theories (Fig. 7 – closed lines). We simulated the rheological behavior of a series of linear polymers on basis of the double reptation model (Thimm et al. 1999) taking into account different degrees of polydispersity. The molecular weights correspond to those of the samples in Fig. 7. The molecular weight distribution was assumed to be of Schulz-Flory type (Soares and Penlidis 2000; Steeman 1998). The shear modulus – phase angle data pairs ($|G^*|$; δ) were calculated from the corresponding $G'(\omega)$ and $G''(\omega)$ data, obtained by means of this simulation. The curves have the same characteristics as those derived experimentally and thus we have shown the applicability of this model which we will need below. As an intermediate result we conclude that the rvGP-plot distinguishes monomodal linear polymers only by their polydispersity.

Bimodality. Mixtures with a linear high and a linear low molecular weight component are important model polymers for understanding the unique course of curve in the vGP-plot. For that reason we considered solution mixed poly(styrene) blends of PS60 as the low molecular weight component and PS644 as the high molecular weight species. The ratio of molar masses is $r = M_w^{hm}/M_w^{lm} = 11$. The blends are denoted by hmPS followed by a number indicating the content of the high molar mass component. Figure 9b shows the rvGP plot of this series. Bimodality causes two minima separated by a maximum. Looking at the G_N^0 region one can see that increasing amounts of high molecular weight species drop the δ values in the G_N^0 minimum, which means that long chains enhance the sample's elasticity. The situation reverses, however, if one moves towards the terminal flow region. Here, for example at a $|G^*|/G_N^0$ ratio of 10^{-2}, the hmPS20 blend has a higher elasticity than the neat high molecular mass species. But this is only a seeming contradiction, since the vGP plot hides the time and length scale information, although they are inherently present. So the different δ_i values (with i being the sample index) in Fig. 9b at a given $|G^*|/G_N^0$ correspond to different states of relaxation. To make this clear we want to focus in the following on the terminal relaxation time λ_T of each sample, that corresponds to identical states of relaxation. A sample's λ_T is identified in Fig. 9a by the intersection point $P_{T,i}$ of the lengthened terminal flow line and the tangent line through the inflection point in the intermediate range. Now we want to locate this point in the rvGP-plot ($P'_{T,i}$ in Fig. 9b) by drawing a vertical line through $P_{T,i}$ across Fig. 9a, b. The intersection between this vertical line and the corresponding curve in Fig. 9b is $P'_{T,i}$. The δ_i values at the corresponding $P'_{T,i}$ points are again a measure of the elasticity affiliated to the same relaxation state. At this point the low molecular weight sample has the lowest elasticity (highest δ); the highest elasticity belongs to the high molar mass probe and the binary blends are in-between. As an interim result we can state here that two relaxation processes with clearly distinct relaxation times can be separated and identified. Moreover, the rvGP-plot is sensitive to species influencing strongly the terminal relaxation time. Only 20% of high molar mass component in a low molecular surrounding (probe hmPS20) practically rule the terminal flow behavior

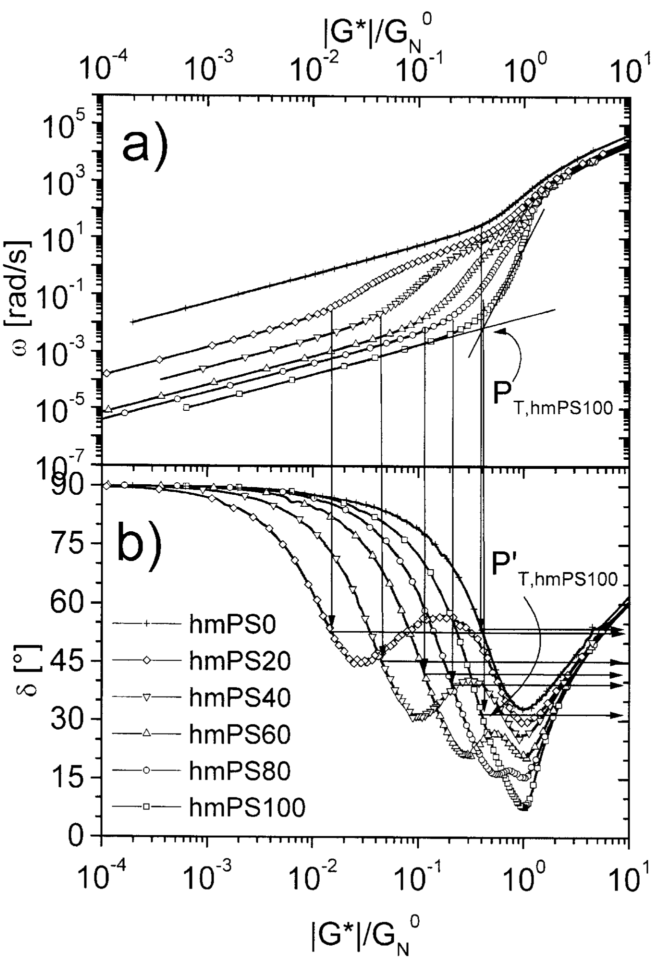

Fig. 9 **a** Experimental data of bimodal poly(styrene)s: ω vs $|G^*|/G_N^0$. The graphs are essentially the G* master curves with interchanged axes. **b** Corresponding RvGP-plots. The abscissas of both plots are identical

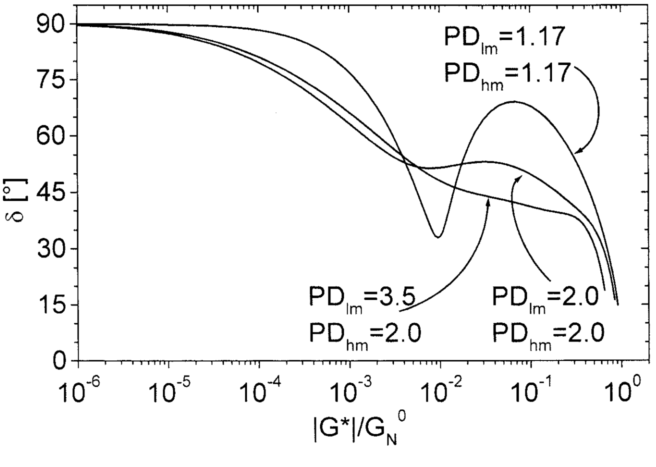

Fig. 10 The influence of the molecular weight distribution of the components for hypothetical bimodal poly(styrene)s with $M_w(\mathrm{lm}) =$ 60 kg/mol and $M_w(\mathrm{hm}) = 644$ kg/mol. The data were simulated applying the double reptation model. Polydispersity is abbreviated by PD

and the left minimum is distinctly developed. In contrast to this, 20% low molar mass chains in a high molar mass matrix (hmPS80) cause only a weak diluting effect and the left minimum is hardly detectable.

At this point we would like to show how polydispersity of the blend components affects the shape of the curve. Since the double reptation model explained above is applicable to our polymer system, we have applied the simulation techniques above explained to answering this question. The hypothetical homopolymer blend was designed to consist of 90 wt% low and 10 wt% high molecular weight species. As the polydispersities (PD in Fig. 10) of the components increase, the left minimum peak becomes less sharp and finally smoothes out. In Fig. 10 the terminal relaxation process remains recognizable even in this case. Obviously, the influence of one distinct species on the terminal relaxation process is not dominant any longer. Important for analysis will be the inverted message: if a second peak is observed in the vGP-plot then an additional distinct species must account for this. Then it is necessary to check the SEC traces for bimodality.

Generalizing these results one can state that each minimum on the left side of the G_N^0 minimum in the van Gurp-Palmen-plot identifies one additional relaxation mode with a clearly distinct relaxation time – regardless of its origin. A minimum at lower $|G^*|/G_N^0$ values belongs to a mode with a longer relaxation time. The more pronounced one species influence over the terminal relaxation process – even if it is present only at low weight percentages – the greater the distances separating the corresponding minima.

Conclusion

In this manuscript we showed that linear polymers can be clearly identified by their characteristic curves in the van Gurp-Palmen-plot. The curves are monotonic at moduli values below G_N^0. Bimodal samples show an additional bump which is due to the relaxation process of the second component in an otherwise monodisperse low molecular weight polymer. In the reduced van Gurp-Palmen-plot (δ; $|G^*|/G_N^0$) structural features like chemical nature, tacticity, and composition in copolymers cancel such that the exact location and width of the curve is primarily governed by the sample's polydispersity. An increasing molar mass distribution leads to a flattening of the curve in a monodisperse sample and in case of bimodality to "smeared" modes. These issues apply to linears. We conclude: if the rvGP plot of a sample has a second mode and bimodality can be excluded then the second relaxation process can be attributed to species with a nonlinear topology. Long chain branching will be addressed in a subsequent article.

Acknowledgements The authors would like to thank A. Eckstein for providing the rheological data of the PS samples, K. Fuchs for the PMMA data, and P. Walter for providing the poly(olefin) samples except the poly(ethene)s that were supplied by A. Köppl, BASF-AG. D. Lilge, BASF-AG, determined the HT-SEC data and the Graduiertenkolleg Strukturbildung in Makromolekularen Systemen funded this work.

References

Doi M, Edwards SF (1986) The theory of polymer dynamics. Oxford Scientific Publications, New York

Donth EJ (1992) Relaxation and thermodynamics in polymers. Akademie Verlag, Berlin

Eckstein A (1998) PhD Thesis, University of Freiburg

Eckstein A, Suhm J, Friedrich C, Maier RD, Sassmannshausen J, Bochmann M, Mülhaupt R (1998) Determination of plateau moduli and entanglement molecular weights of isotactic, syndiotactic and atactic polypropylenes synthesized with metallocene catalysts. Macromolecules 31:1335–1340

Ferry JD (1980) Viscoelastic properties of polymers, 3rd edn. Wiley, New York

Fetters J, Lohse DJ, Graessley WW (1999) Chain dimensions and entanglement spacings in dense macromolecular systems. J Polym Sci Polym Phys 37: 1023–1033

Fuchs K, Friedrich C, Weese J (1996) Viscoelastic properties of narrow-distribution poly(methylmethacrylate)s. Macromolecules 29:5893–5901

Honerkamp J, Weese J (1993a) A note on estimating mastercurves. Rheol Acta 32:57–64

Honerkamp J, Weese J (1993b) A nonlinear regularization method for the calculation of relaxation spectra. Rheol Acta 32:65–73

Kazatchkov B, Bohnet N, Goyal SK, Hatzikiriakos SG (1999) Influence of molecular structure on the rheological and processing behavior of polyethylene resins. Polym Eng Sci 39(4): 804–815

Lobbrecht A, Friedrich C, Sernetz FG, Mülhaupt R (1997) Viscoelastic properties of poly(ethylene-*co*-styrene) copolymers. J Appl Polym Sci 65:209–215

Mavridis H, Shroff RN (1992) Temperature dependence of polyolefin melt rheology. Polym Eng Sci 32(23):1778–1791

Soares JBP, Penlidis A (2000) Measurement, mathematical modelling and control of distribution of molecular weight, chemical composition and long-chain branching of polyolefins made with metallocene catalysts. In: Scheirs J, Kaminsky W (eds) Metallocene-based polyolefins: preparation, properties and technologies, vol 2. Wiley, Chichester, p. 237

Steeman PAM (1998) A numerical study of various rheological polydispersity measures. Rheol Acta 37:583–592

Suhm J (1998) PhD Thesis, University of Freiburg

Thimm W, Friedrich C, Marth M, Honerkamp J (1999) An analytical relation between relaxation time spectrum and molecular weight distribution. J Rheol 43:1663–1672

Van Gurp M, Palmen J (1998) Time temperature superposition for polymeric blends. Rheol Bull 67:5–8

Walter P (1998) Diploma Thesis, University of Freiburg

Wu S, Beckerbauer R (1992) Chain entanglement in homopolymers, copolymers and terpolymers of methylmethacrylate, styrene and *N*-phenylmaleimide. Polymer 33:509–515